





Enhanced reliability and time efficiency of deep learning-based posterior tibial slope measurement over manual techniques

Shang-Yu Yao¹  | Xue-Zhi Zhang² | Soumyajit Podder³  | Chen-Te Wu⁴  |
Yi-Shen Chan^{1,5,6}  | Dan Berco^{5,7} | Cheng-Pang Yang^{1,5} 

¹Department of Orthopedic Surgery, Linkou Chang Gung Memorial Hospital, Taoyuan City, Taiwan

²Engineering Product Development, Singapore University of Technology and Design, Tampines, Singapore

³Department of Biomedical Engineering, Chang Gung University, Taoyuan City, Taiwan

⁴Department of Medical Imaging and Intervention, Linkou Chang Gung Memorial Hospital, Taoyuan City, Taiwan

⁵Comprehensive Sports Medicine Center, Taoyuan Chang Gung Memorial Hospital, Taoyuan City, Taiwan

⁶Department of Orthopedic Surgery, Keelung Chang Gung Memorial Hospital, Keelung City, Taiwan

⁷Department of Electronics Engineering and Program in Nano-Electronic Engineering and Design, Chang Gung University, Taoyuan City, Taiwan

Correspondence

Cheng-Pang Yang, Department of Orthopedic Surgery, Linkou Chang Gung Memorial Hospital, No. 5, Fuxing St, Guishan, Taoyuan City 333, Taiwan.
Email: ronnie80097@gmail.com

Dan Berco, Department of Electronics Engineering and Program in Nano-Electronic Engineering and Design, Chang Gung University, No. 259 Wenhua 1st Rd, Guishan, Taoyuan City 333, Taiwan.
Email: danny@mail.cgu.edu.tw

Funding information

National Science and Technology Council (NSTC) of Taiwan, Grant/Award Numbers: 112-2221-E-182-060, 112-2813-C-182A-002-B

Abstract

Purpose: Multifaceted factors contribute to inferior outcomes following anterior cruciate ligament (ACL) reconstruction surgery. A particular focus is placed on the posterior tibial slope (PTS). This study introduces the integration of machine learning and artificial intelligence (AI) for efficient measurements of tibial slopes on magnetic resonance imaging images as a promising solution. This advancement aims to enhance risk stratification, diagnostic insights, intervention prognosis and surgical planning for ACL injuries.

Methods: Images and demographic information from 120 patients who underwent ACL reconstruction surgery were used for this study. An AI-driven model was developed to measure the posterior lateral tibial slope using the YOLOv8 algorithm. The accuracy of the lateral tibial slope, medial tibial slope and tibial longitudinal axis measurements was assessed, and the results reached high levels of reliability. This study employed machine learning and AI techniques to provide objective, consistent and efficient measurements of tibial slopes on MR images.

Results: Three distinct models were developed to derive AI-based measurements. The study results revealed a substantial correlation between the measurements obtained from the AI models and those obtained by the orthopaedic surgeon across three parameters: lateral tibial slope, medial tibial slope and tibial longitudinal axis. Specifically, the Pearson correlation coefficients were 0.673, 0.850 and 0.839, respectively. The Spearman rank correlation coefficients were 0.736, 0.861 and 0.738, respectively. Additionally, the interclass correlation coefficients were 0.63, 0.84 and 0.84, respectively.

Conclusion: This study establishes that the deep learning-based method for measuring posterior tibial slopes strongly correlates with the evaluations of expert orthopaedic surgeons. The time efficiency and consistency of this technique suggest its utility in clinical practice, promising to enhance workflow, risk assessment and the customization of patient treatment plans.

Level of Evidence: Level III, cross-sectional diagnostic study.

Abbreviations: ACL, anterior cruciate ligament; AI, artificial intelligence; CI, confidence interval; CT, computed tomography; ICC, interclass correlation coefficient; IQR, interquartile range; mAP, mean average precision; MRI, magnetic resonance imaging; PD, proton density; PTS, posterior tibial slope; SD, standard deviation; SGD, stochastic gradient descent; TE, echo time; TR, repetition time; YOLO, you only look once.

Shang-Yu Yao, Xue-Zhi Zhang, and Soumyajit Podder contributed equally to this study and as first authors.

© 2024 European Society of Sports Traumatology, Knee Surgery and Arthroscopy.

KEYWORDS

anterior cruciate ligament, artificial intelligence, automated measurements, deep learning, posterior tibial slope

INTRODUCTION

Multiple factors contribute to inferior outcomes or complications following anterior cruciate ligament (ACL) reconstruction surgery, which include anatomical variations, neuromechanical elements, biomechanical movements, genetics and hormonal influences [6, 27, 28]. One particularly relevant knee morphological factor is the posterior tibial slope, which significantly impacts anterior-posterior stability, mechanical tension on the ACL and anterior shearing forces [7, 12]. The posterior tibial slope (PTS) consists of both the lateral tibial slope and the medial tibial slope, both are intricately linked to the ACL [16, 18, 33]. Prior meta-analyses and systematic reviews have firmly established the connection between an increased PTS and primary ACL injury [4, 29, 33, 35, 36]. Furthermore, other studies underscore the correlation between elevated PTS and ACL graft rupture or reconstruction failure, emphasizing its prognostic value in patients who underwent ACL repair [8, 11, 13, 14]. Notably, the PTS also plays a pivotal role in surgical planning for other knee procedures, such as high tibial osteotomy and total knee arthroplasty, as an inadequate slope can lead to postoperative knee instability and inferior outcomes [10, 15]. These investigations underscore the pronounced clinical relevance of the posterior tibial slope.

Despite advancements in diagnostic modalities, including plain radiographs, computed tomography (CT) and magnetic resonance imaging (MRI), the discrepancies in measuring tibial slopes persist [10, 15, 17, 32, 37]. A meta-analysis conducted by Wang et al. revealed a range of mean medial tibial slopes from 1.8° to 13.2° and mean lateral tibial slopes from 1.2° to 9° among individuals with ACL injuries [33]. Another systematic review by Liu et al. highlighted the vast disagreement in tibial slope measurements, despite the availability of highly reliable measuring techniques [19]. A comparative cross-sectional study by Naendrup et al. further demonstrated the pronounced variability and inaccuracy between different imaging modalities and measuring methods for posterior tibial slopes [23].

While MRI excels in measuring lateral and medial tibial slopes compared to traditional 2D methods, those challenges remain. Despite efforts by Hudek et al. and Hashemi et al. to address measurement challenges, intraobserver and interobserver variabilities persist, impacting reliability [15, 17, 30]. These errors came from either the selection of appropriate sagittal slices or the subjective nature of the measuring techniques used

[2]. Accordingly, surgeons and researchers are facing challenges in establishing certain values for risk stratification, clinical recommendations and pre-operative planning. Furthermore, advancements in diagnostic and imaging technologies have increased the workload for medical practitioners, necessitating a thorough analysis of voluminous data sets.

The focus of this study is the application of deep learning approaches to tibial slope measurement in MR images, which emerges as a promising solution. By accurately identifying specific landmarks on MR images, this method has the potential to introduce objectivity, consistency and efficiency in tibial slope measurements. It is hypothesized that the deep learning-based model will not only demonstrate a high correlation with manual measurements conducted by experienced orthopaedic surgeons but also excel in terms of consistency and reliability.

MATERIALS AND METHODS

Data acquisition and study design

This project involved 120 patients who underwent ACL reconstruction surgery in the past 10 years at Chang Gung Memorial Hospital. Ethical approval for the study was obtained from the Institutional Review Board of the Chang Gung Memorial Hospital (Number: 202200726B0). The medical images, retrieved from the hospital's electronic medical records, were complemented by demographic information, including age, gender, injury side, body weight and height. The exclusion criteria included prior surgery, high-grade osteoarthritis, incomplete medical records, incomplete imaging studies, bone fractures or artificial implants.

The parameters analysed in this study were the lateral tibial slope, medial tibial slope and tibial longitudinal axis. The measuring technique used for this study was modified from the one proposed by Hudek et al. [17]. The traditional Hudek method involves drawing a tangent line across the uppermost edges of the tibial plateau, which can be challenging due to the anatomical variability among patients, especially those with a rounded tibial plateau. Apart from the anatomical variability, it is noteworthy that even among well-trained orthopaedic surgeons, some degree of inconsistency in measuring tibial slopes using the Hudek method exists [2]. The AI model introduces a novel methodology by utilizing bounding boxes to delineate the meniscus on sagittal MRI images, thereby calculating the meniscal

slope by the centre of the boxes. For the tibial longitudinal axis, the concept of the cranial circle was preserved but the caudal circle was replaced with a bounding box. This bounding box is designed to align with the image's lower edge, ensuring it captures the widest possible expanse of the visible tibial bone, which presents the geometric centre of the lower tibia. The integration of these modifications was aimed at refining the AI system, wherein the simplification of its design was pursued to enhance stability and reliability. It was hypothesized that the system could yield results closely mirroring the established Hudek method, despite variations in methodology.

MRI techniques were employed to assess tibial slope measurements. Knee MRI scans were conducted using a 3.0 Tesla scanner with a slice thickness of 4 mm, and the images were processed using Centricity PAC. All MRI images were acquired utilizing a proton density (PD) weighted sequence to enhance the visibility of the ACL ligaments and meniscus cartilage. The imaging protocol included the acquisition of axial, sagittal and coronal series to comprehensively capture the knee anatomy. The subjects were placed in a supine position, ensuring an unloaded knee and a neutral alignment during the collection of images. Specific sagittal image slices were manually selected by an orthopaedic resident and subsequently verified by a supervising orthopaedic surgeon for artificial intelligence model training and assessment. The central sagittal image, crucial for defining the mechanical axis, is identified based on the presence of key anatomical landmarks, including the tibial attachment of the Posterior Cruciate Ligament (PCL), the intercondylar eminence and the concave appearance of the anterior and posterior tibial cortices. The centres of the medial plateau and lateral plateau are identified through cross-referencing of axial and sagittal images. Two methods, the AI-based model and manual measurement by an experienced orthopaedic surgeon using Hudek's technique, were employed for parameter measurements.

The computational tool developed during this study is an AI-based neural network capable of detecting and measuring the tibial slope. This was instrumental not only in ascertaining the fidelity of the PTS measurements but also in acting as a performance benchmark in later stages. In this phase, an advanced programming language, namely Python, was utilized for algorithmic development. Three different AI models were created to measure the lateral tibial slope, medial tibial slope and tibial longitudinal axis, respectively. Subsequently, the AI-based neural network was subjected to both training and performance evaluation processes using real-world medical data sets. The necessity for an AI-driven automated methodology for the assessment of tibial slope measurements in knee MRI was identified as a crucial requirement. For this

purpose, a supervised learning framework was meticulously designed with the consultation of medical experts.

Preprocessing and model training

The project involved 120 patients with complete knee MRI series. To develop the model, images from 80 patients were employed in the training phase. The images from the remaining 40 patients were utilized to evaluate the reliability of the model. The images obtained from the slices were in DICOM 3.0 format (.dcm) format and were converted into jpg format for further processing. In this study, the model training and automatic detection were conducted employing YOLOv8, a state-of-the-art algorithm renowned for its object detection and instance segmentation capabilities. It employs a single neural network that delivers the bounding box's coordinates and its category prediction. More flexible deployment and precise detection can be achieved due to more compact and practical features of the model, compared to previous algorithms. To prevent issues of overfitting, data augmentation was employed to gather additional information for the training of the model. To acquire more meaningful data, different augmentation techniques such as rotation, flipping, resizing and Gaussian blurring were specifically employed.

Lateral and medial tibial slope measurement method

The YOLOv8 model was utilized for the detection of the lateral meniscus and articular cartilage from hospital patient data. The parts marked during the annotation of the image region are the lateral meniscus and medial meniscus. The rectangular bounding boxes to annotate the data set with category and coordinate information were performed by a programme known as labelling by skilled radiologists. For the investigation of the tibial slope, two bounding boxes of the same class were considered to label the menisci. The images were trained on a workstation in a Python environment on a Windows system with an NVIDIA RTX 3080 Ti with 16 GB RAM and Intel Core i9 12th generation @2.5 GHz processor. The MRI images used for this clinical study were high resolution (918×918) and were proton density (PD)-weighted images. The YOLOv8 algorithm was trained on 80 sets of images for 100 epochs with batch sizes of 16 from different patient groups. The best model weights were saved, the results were inferred from the test set, and the tibial slope and longitudinal axis were calculated consequently from them. The network is constructed using the open-source PyTorch (GPU) framework and is

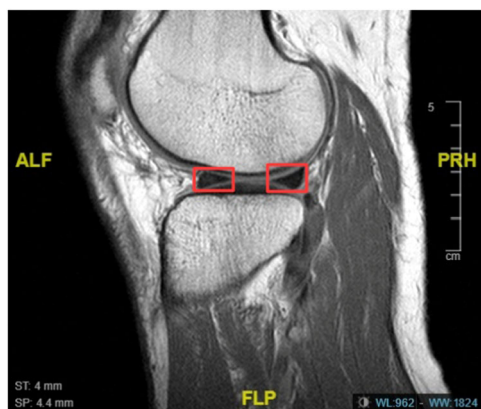


FIGURE 1 Image labelling for the lateral tibial slope measurement. The figure demonstrates the artificial intelligence model's autonomous detection of the meniscus at the centre of the lateral tibial plateau on sagittal magnetic resonance imaging images. ALF, anterior lateral femur; FLP, femorolateral posterior; PRH, posterior right horn.

optimized with the Stochastic Gradient Descent (SGD) optimizer for enhanced model performance. The learning rate decay value of the SGD optimizer is set to 0.01 following each training and gradient update. The hyperparameters included setting the momentum to 0.937 and weight decay to 0.0005.

After applying the trained YOLOv8 model on test images, the model will draw two boxes automatically around the meniscus and provide the coordinates of the centre of the boxes, respectively, illustrated in Figure 1. With the given coordinates from the outputs of the test process, the programme calculates the gradient of the line formed by the two points, with respect to the universal coordinates of the image, and plots a line for reference. A reference line is then plotted on the image based on this gradient, serving as a visual aid to review the results obtained from the AI model. The calculated angle between this reference line and the horizontal axis is mathematically defined as the tibial slope, with an accuracy of ± 0.01 degrees. To validate the accuracy of this measurement, the comparison is made with tibial slope data obtained through manual drawing by medical personnel.

Tibial longitudinal axis measurement method

The bounding box detection was used to locate the five positions around the Tibia bone out of which three positions were used to draw the final circle, while the bottommost position was used to detect the midpoint of the longitudinal axis. The unused boxes while drawing the circle are shown in Figure 2. The training process with more boxes has better performance in eliminating the possibility of the programme for the recognition of the false positive during detection. The unwanted

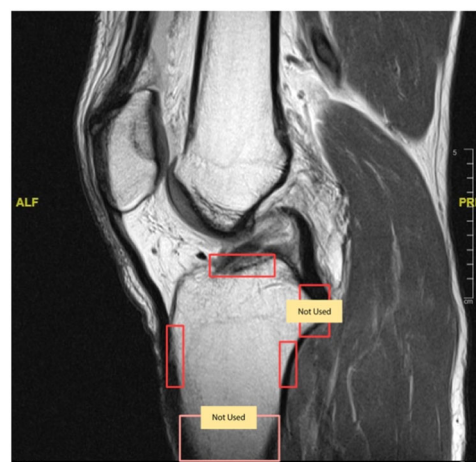


FIGURE 2 Image labelling for the tibial longitudinal axis measurement. The figure illustrates the artificial intelligence's application of bounding boxes to identify critical points for creating the cranial circle, aligning with the modified Hudek technique. Excess boxes, while not used in the final evaluation to maintain precision and reduce false detections, are filtered out after the training phase. ALF, anterior lateral femur; PRH, posterior right horn.

coordinates were automatically eliminated by the programme later. The model was trained on the YOLOv8 algorithm for 100 epochs the same as before. Since YOLOv8x can identify objects with high accuracy, performs well in real-time and can be trained on bespoke data sets with flexibility, it was chosen as the pretrained model for training on knee MR images.

The top corner of the point where it first starts to curve in the anterior and posterior tibial cortex and the cartilage is marked for training. The resultant bounding box coordinates were used as a reference to draw the circle. The circle is plotted from the bottom middle point of the top box, from the leftmost middle point of the left box and the middle point of the rightmost box. With three sets of coordinates and the general circle equation, $(x - h)^2 + (y - k)^2 = r^2$, the centre point and radius of the circle can be plotted by putting in the coordinates. The caudal circle of the Hudek method is replaced by a bounding box designed to align with the image's lower edge, ensuring it captures the widest possible expanse of the visible tibial bone. A reference line is then plotted using the centre of the circle and the centre of the lower bounding box. The tibial longitudinal axis is determined by the angle between the reference line and the horizontal axis, calculated mathematically with a precision of ± 0.01 degrees.

Statistical analysis

The results from the newly designed AI-based technique were compared with those of the orthopaedic surgeon, considered as the gold standard in this study.

Statistical tests were conducted using SPSS 28.0 (SPSS), which included the student *T*-test, Pearson's correlation coefficient, Spearman's rank correlation coefficient and Interclass correlation coefficient (ICC). Due to the absence of a universally accepted gold standard for the posterior tibial slope, evaluating the absolute accuracy of the AI model's results poses challenges. Nevertheless, the primary objective of the model is to achieve a strong correlation with human measurement results and replace the laborious clinical task of tibial slope measurement. Test–retest reliability measurement was not conducted in this study since the AI-based automated method consistently yielded the same results, surpassing human capabilities without errors.

RESULTS

A total of 120 patients were enrolled and their knee MRI series were analysed. The MR images were randomly split into training and test data set ratios of 2:1. Of the 120 patient image samples with medical records, 80 were used to train the artificial intelligence model, and 40 were used to test the model. Three different models were created for measuring the lateral and medial tibial slope and the tibial longitudinal axis. This process resulted in 240 images for the lateral and medial tibial slope and 120 images for the longitudinal axis, respectively. The identities of the patients were withheld for ethical concerns. No other disease diagnosis was believed to affect the study via careful review of the images.

The accuracy of the AI model for correctly labelling the box with the tibial slope is 99.8% while the accuracy of the longitudinal axis is 99.3%. Mean Average Precision (mAP) is a crucial metric in detection that provides a single figure that encapsulates the performance of a model across all classes and object instances. Higher mAP scores signify enhanced accuracy and error minimization. The model reached a mAP value of 99.5% upon validation of the data set for both experiments. The system had reached high mAP utilizing imagery from 80 patients, concluding that the addition of MR images to the training set does not markedly improve the algorithm's performance. The bounding boxes were obtained with high accuracy and specificity. More MRI data can be added to further improve the performance of the pre-trained model. The results obtained from the images were compared across different parameters such as age, gender, height, weight and injury side. The results were validated and were found to be reliable even with repeated tests by the AI model. The tibial slope inferred by the AI model was compared with the doctor's measured tibial slope as illustrated in Figure 3. The blue line shows the slope obtained from the AI and the orange line illustrates the manually labelled data. The tibial longitudinal axis is measured from the gradient of

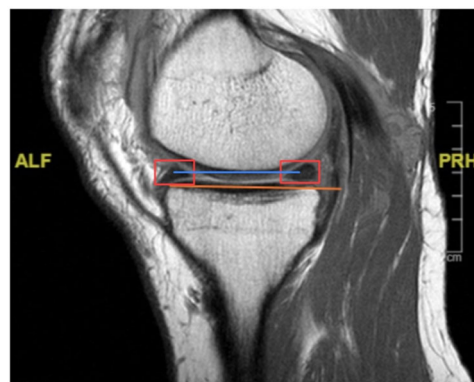


FIGURE 3 Line plotted for results comparison between artificial intelligence (AI) and orthopaedic surgeon measurement of medial tibial slope. The figure depicts the comparison of tibial slope measurements. The figure illustrates the AI-generated line in blue is derived from the centres of the bounding boxes, while the manually measured line by the orthopaedic surgeon is shown in orange. ALF, anterior lateral femur; PRH, posterior right horn.



FIGURE 4 Circle and corresponding line plotted for results comparison between artificial intelligence (AI) and orthopaedic surgeon measurement of tibial longitudinal axis. The comparison of tibial longitudinal axis measurement. The figure presents the AI's version is delineated in blue, while the orthopaedic surgeon's manual measurement is indicated in yellow.

the line calculated from the centre of the circle to the centre of the bottom box. A circle has been plotted on the image from the three boxes; the blue line indicates the tibial longitudinal axis determined by the AI model, while the green line illustrates the manually measured data as shown in Figure 4.

Comparative analysis of AI and manual measurement techniques

The investigation of the ability of the AI system to automatically measure posterior tibial slopes in

orthopaedic patients yielded several notable outcomes. From the 40 samples tested, the AI measurements were compared with those obtained by an experienced orthopaedic surgeon across three parameters: lateral tibial slope, medial tibial slope and tibial longitudinal axis. The analysis focused on tibial slopes and the longitudinal axis, and the outliers were diligently identified and excluded based on the interquartile range (IQR) methodology. Only one outlier was identified in the medial tibial slope and removed. Patients with missing values due to limitations of the AI model were also removed. The final data set consisted of 40 patients in the lateral tibial slope group, 39 in the medial tibial slope group and 27 in the tibial longitudinal axis group.

Descriptive statistics

Table 1 illustrates the differences in the measurements between the orthopaedic surgeon and the AI model. The orthopaedic surgeon's assessment of the lateral tibial slope yielded an average value of -3.74 ± 1.12 , whereas the average of the AI system's estimation was 0.62 ± 1.62 . Similarly, the orthopaedic surgeon's measurements averaged at -3.40 ± 1.37 for the medial tibial slope, in contrast to the AI mean value of -1.08 ± 1.59 . Delving into the tibial longitudinal axis, the surgeon's measurements averaged 93.51 ± 1.31 , while the AI's measurements were approximately 93.68 ± 1.34 . Notably, statistical evaluation through paired *T*-test highlighted significant differences between the orthopaedic surgeon's and the AI system's measurements across all three parameters, with *p*-values consistently less than 0.05. This emphasizes the inherent disparities between human expertise and AI-driven determinations.

Correlation analysis

Table 2 displays the correlation analysis between the measurements taken by orthopaedic surgeons and those generated by an AI model. Additionally,

Figures 5–7 provide scatterplot visualizations for a clearer representation of the data.

a. Lateral tibial slope

A distinct positive linear correlation was observed, with a Pearson correlation coefficient of 0.694. The Spearman rank coefficient further reinforced this trend, with a value of 0.851. The ICC was 0.630. Taken together, the correlation analysis showed a moderate correlation between the two methods.

b. Medial tibial slope

The Pearson correlation coefficient of 0.850 revealed a strong positive linear relationship. An even stronger Spearman rank correlation of 0.862 was noted. The ICC was also high at 0.84 (0.72, 0.91, two-way fixed), suggesting a strong correlation between the AI's and the surgeon's measurements of the medial tibial slope.

c. Tibial longitudinal axis

A strong positive linear relationship was indicated by a Pearson correlation coefficient of 0.839. The Spearman rank correlation was slightly weaker at 0.738. The ICC was 0.838 (0.68, 0.92, two-way fixed), denoting strong consistency between the two measurement techniques.

TABLE 2 Correlation analysis between the measurements of an orthopaedic surgeon and artificial intelligence (AI) model.

Measurement parameters	Pearson	Spearman	ICC [95% confidence interval]
Lateral tibial slope (<i>n</i> = 40)	0.67	0.74	0.63 [0.40–0.79]
Medial tibial slope (<i>n</i> = 39)	0.85	0.86	0.84 [0.72–0.91]
Tibial longitudinal axis (<i>n</i> = 27)	0.84	0.74	0.84 [0.68–0.92]

Note: The table summarizes the correlation coefficients for lateral and medial tibial slopes and the tibial longitudinal axis, comparing results from the orthopaedic surgeon with those generated by the AI model. Pearson's and Spearman's coefficients provide insights into linear and rank-order relationships, respectively, while the interclass correlation coefficient (ICC) with 95% confidence intervals assesses the consistency between the two measurement methods.

TABLE 1 Differences between the measurements of an orthopaedic surgeon and the artificial intelligence (AI) model.

Measurement parameters	Surgeon Mean (±SD)	AI Mean (±SD)	Difference <i>p</i> -Value	[95% CI]
Lateral tibial slope (<i>n</i> = 40)	−3.74 (±1.12)	0.62 (±1.62)	<0.001	[3.12–5.59]
Medial tibial slope (<i>n</i> = 39)	−3.40 (±1.37)	−1.08 (±1.59)	<0.001	[2.34–3.59]
Tibial longitudinal axis (<i>n</i> = 27)	93.51 (±1.31)	93.68 (±1.34)	0.66	[1.20–2.09]

Note: The table compares the mean and standard deviation (SD) of lateral and medial tibial slopes and the tibial longitudinal axis measurements obtained by the orthopaedic surgeon against those derived from the AI model. Statistical significance is determined by paired *T*-test *p*-values, and the range of measurement differences is captured within 95% confidence intervals (CIs).

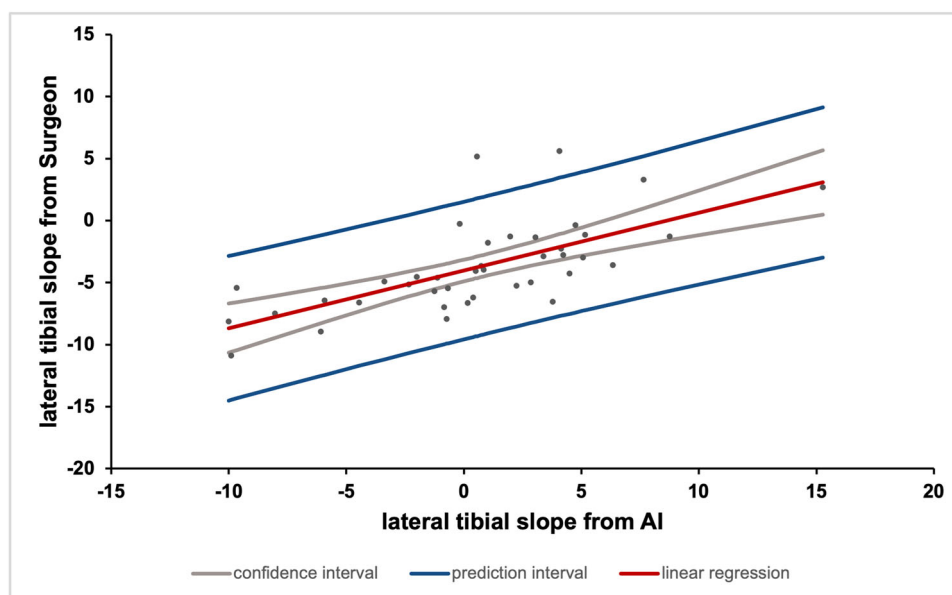


FIGURE 5 Scatterplot of the lateral tibial slope model. The figure compares the measurements of lateral tibial slope as obtained by the artificial intelligence (AI) model versus the orthopaedic surgeon. The red lines represent linear regression, indicating the trend of the relationship. Grey lines depict the confidence intervals around the regression lines, estimating their precision, while blue lines show the prediction intervals, indicating where future measurements may be expected to fall.

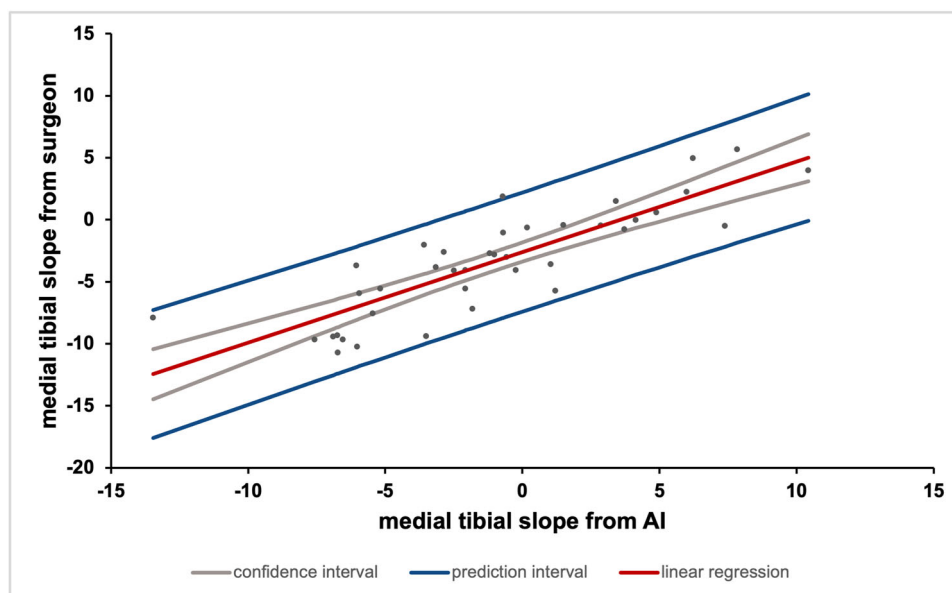


FIGURE 6 Scatterplot of the medial tibial slope model. The figure compares the measurements of medial tibial slope as obtained by the artificial intelligence (AI) model versus the orthopaedic surgeon. The red lines represent linear regression, indicating the trend of the relationship. Grey lines depict the confidence intervals around the regression lines, estimating their precision, while blue lines show the prediction intervals, indicating where future measurements may be expected to fall.

In conclusion, a moderate to strong correlation was detected between the AI model's measurements and those of the orthopaedic surgeon in all three parameters. This indicates that an exact translation equation between the two measurement results may be discovered in future studies. However, this approach may not involve a simple direct linear approach or a fixed difference.

DISCUSSION

The most important finding of the present study is that the artificial intelligence-based model exhibits a moderate to high correlation with manual measurements conducted by an experienced orthopaedic surgeon. While there are notable differences between human

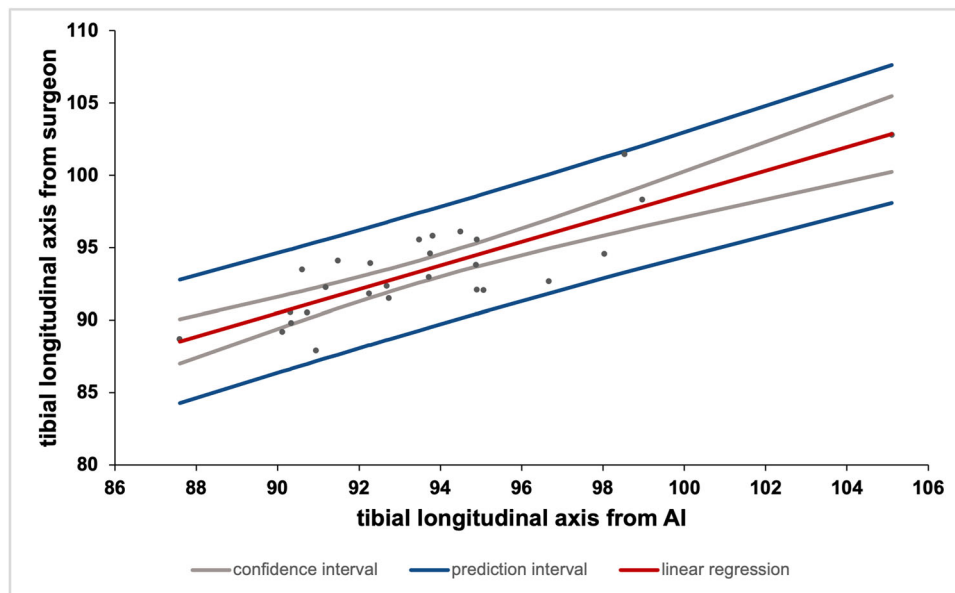


FIGURE 7 Scatterplot of the tibial longitudinal axis model. The figure compares the measurements of tibial longitudinal axis as obtained by the artificial intelligence (AI) model versus the orthopaedic surgeon. The red lines represent linear regression, indicating the trend of the relationship. Grey lines depict the confidence intervals around the regression lines, estimating their precision, while blue lines show the prediction intervals, indicating where future measurements may be expected to fall.

assessments and AI-driven results across all three measured parameters, largely attributable to methodological adjustments, the significant correlation underscores the potential for developing a precise translation equation between the two sets of measurements in future research.

The ACL rupture, a common debilitating knee injury, is potentially influenced by posterior tibial slopes [7, 9]. It was reported in previous studies that higher slopes correlate with increased preoperative laxity in ACL-injured patients and suboptimal postreconstruction outcomes [1, 5, 26]. Therefore, identifying a tibial slope threshold that elevates the risk of ACL rupture is crucial. Yet, the establishment of a universally accepted standard for measuring lateral and medial tibial slopes remains elusive [21].

Traditional methods for measuring tibial slopes, such as those by Hashemi et al. and Hudek et al., [15, 17] exhibit significant variability due to operator dependence. This is evident in the inconsistent intraobserver and interobserver reliability in clinical practice, with reported ranges of mean medial tibial slopes in ACL-injured individuals ranging from 4.7 to 11.2 and lateral tibial slopes ranging from 5.6 to 9, as indicated by previous meta-analyses [2, 22]. In contrast, the AI approach offers a more objective and reliable alternative. The tool harnesses Hudek's methodology, renowned for its accuracy in traditional practices, to define the tibial longitudinal axis. Additionally, the AI model's capacity to consistently reproduce results on identical images significantly enhances its reliability. Furthermore, the potential of the AI model to

increase precision and its adaptability through expanded training data sets highlights its advantages.

Several studies have explored the use of computer programming languages and 3D methodologies for automated tibial slope measurements. Amerinatanzi et al. developed a MATLAB-based approach, utilizing MRI planar images to measure tibial slopes. Their method involved outlining the lateral and medial condyle contours and employing Gaussian curvature analysis. The system demonstrated efficiency, delivering results for the lateral tibial slope, medial tibial slope and coronal tibial slope in just 20 s [2]. Similarly, Amirtharaj et al. introduced a MATLAB-based approach for identifying lateral tibial slopes using 3D reconstructed computer tomography (CT) scans of the proximal tibia [3]. The tibial longitudinal axis was computed through principal component analysis, and the lateral tibial slope was determined by fitting a plane to points outlining the lateral rim of the tibial plateau. While both studies demonstrated excellent reliability and consistency in measuring tibial slopes, a notable limitation is the absence of comparisons to manual measurement results in real-world data, raising questions about their clinical impact. Furthermore, the fixed code in these approaches limits adjustability and potential algorithmic improvements, especially with larger databases.

In contrast, the approach of utilizing artificial intelligence and machine learning represents a novel direction in the field, which has been previously explored in several studies. This strategy not only maintains the strengths of automated measurement

techniques but also holds promise for enhancing the measuring algorithm over time. Tong et al. have developed a RetinaNet-based tool that assists in the measurement of the posterior tibial slope by accurately labelling the region of interest in X-ray images [31]. Lu et al. implemented a deep learning-based method directly measuring posterior tibial slope on X-ray images, which has shown significant concordance with manual evaluations conducted by orthopaedic residents [20]. Notably, these studies have exclusively focused on measurements from plain radiographs. The system we introduced enhances these capabilities by independently measuring both lateral and medial slopes on MR images. In clinical settings, such a system could assist orthopaedic surgeons in rapidly measuring tibial slopes with high consistency, thereby replacing the traditional method, which is time-consuming and relatively subjective. The configuration of the algorithm can be achieved with minimal computational effort, making it appropriate for environments constrained by computational resources. This advancement could improve preoperative risk stratification and postoperative prognostic value for ACL injury cases, leading to more individualized treatment strategies.

There were several limitations to this study. First, patient variability in knee orientations led to inconsistencies in MRI sagittal cuts and the manual selection of image slices for measurements introduced subjectivity and potential errors [2]. Second, the training images were derived from ACL-injured patients, potentially not fully reflecting normal knee anatomy. The inclusion of patients with ACL injury-related bone bruises or low-grade osteoarthritis during training might have impacted the accuracy of the model. Moreover, the AI model encounters challenges in accurately measuring images affected by extensive meniscus damage, insufficient proximal tibial shaft length or incomplete bone cortex borders. Additionally, relying on measurements obtained by orthopaedic specialists as a gold standard raises concerns about the true accuracy of the proposed method. Alternatives such as 2D radiographs, CT images or cadaveric tibia measurements, while potentially more objective, also pose their limitations and practical challenges [24, 25, 34]. Therefore, establishing a more objective gold standard for tibial slope measurements emerges as a critical area for future research. Addressing these limitations will contribute to the refinement and broader applicability of our proposed method, fostering its potential for clinical use.

CONCLUSION

In conclusion, the study demonstrates that the artificial intelligence-based method of posterior tibial slope measurement yields results highly correlated with manual measurements by experienced orthopaedic

surgeons. Time efficiency and reproducibility of this AI-based approach make it a valuable tool for daily clinical practice, offering benefits in terms of streamlined workflows, improved risk stratification and individualized treatment plans for ACL-injured patients.

AUTHOR CONTRIBUTIONS

Shang-Yu Yao: Conceptualization; investigation; methodology; formal analysis; visualization; writing—original draft, writing—review and editing. **Xue-Zhi Zhang:** Conceptualization; data curation; methodology; software; validation; writing—review and editing. **Soumyajit Podder:** Conceptualization; data curation; methodology; software; validation; writing—review and editing. **Chen-Te Wu:** Conceptualization; resources; methodology. **Yi-Shen Chan:** Conceptualization; resources; supervision. **Dan Berco:** Conceptualization; methodology; supervision. **Cheng-Pang Yang:** Conceptualization; methodology; supervision.

ACKNOWLEDGEMENTS

The authors acknowledge the funding support by the National Science and Technology Council (NSTC) of Taiwan under grant 112-2221-E-182-060 and 112-2813-C-182A-002-B.

CONFLICT OF INTEREST STATEMENT

The authors declare no conflict of interest.

DATA AVAILABILITY STATEMENT

All relevant data required for training and testing of the AI model can be found at Open Science Framework (<https://osf.io/5tazu/>), following an embargo from the date of publication to allow for commercialization of research findings.

ETHICS STATEMENT

Ethical approval for the study was obtained from the Chang Gung Medical Foundation Institutional Review Board (Number: 202200726B0). Patient consent was waived due to ethical clearance by the Linkou Chang Gung Memorial Hospital when using anonymized clinical data for the retrospective analysis.

ORCID

Shang-Yu Yao  <http://orcid.org/0009-0009-9907-3990>

Soumyajit Podder  <https://orcid.org/0000-0002-1113-5299>

Chen-Te Wu  <http://orcid.org/0000-0001-7161-6740>

Yi-Shen Chan  <http://orcid.org/0000-0001-7413-1431>

Cheng-Pang Yang  <http://orcid.org/0009-0007-8547-4561>

REFERENCES

1. Ahmed, I., Salmon, L., Roe, J. & Pinczewski, L. (2017) The long-term clinical and radiological outcomes in patients who

- suffer recurrent injuries to the anterior cruciate ligament after reconstruction. *The Bone & Joint Journal*, 99-b, 337–343. Available from: <https://doi.org/10.1302/0301-620X.99B3.37863>
2. Amerinatanzi, A., Summers, R.K., Ahmadi, K., Goel, V.K., Hewett, T.E. & Nyman, E. (2017) Automated measurement of patient-specific tibial slopes from MRI. *Bioengineering (Basel)*, 4, 69. Available from: <https://doi.org/10.3390/bioengineering4030069>
 3. Amirtharaj, M.J., Hardy, B.M., Kent 3rd, R.N., Nawabi, D.H., Wickiewicz, T.L., Pearle, A.D. et al. (2018) Automated, accurate, and three-dimensional method for calculating sagittal slope of the tibial plateau. *Journal of Biomechanics*, 79, 212–217. Available from: <https://doi.org/10.1016/j.jbiomech.2018.07.047>
 4. Bayer, S., Meredith, S.J., Wilson, K.W., de Sa, D., Pauyo, T., Byrne, K. et al. (2020) Knee morphological risk factors for anterior cruciate ligament injury: a systematic review. *Journal of Bone and Joint Surgery*, 102, 703–718. Available from: <https://doi.org/10.2106/JBJS.19.00535>
 5. Beel, W., Schuster, P., Michalski, S., Mayer, P., Schlumberger, M., Hielscher, L. et al. (2023) High prevalence of increased posterior tibial slope in ACL revision surgery demands a patient-specific approach. *Knee Surgery, Sports Traumatology, Arthroscopy*, 31, 2974–2982. Available from: <https://doi.org/10.1007/s00167-023-07313-2>
 6. Boden, B.P., Sheehan, F.T., Torg, J.S. & Hewett, T.E. (2010) Noncontact anterior cruciate ligament injuries: mechanisms and risk factors. *American Academy of Orthopaedic Surgeon*, 18, 520–527. Available from: <https://doi.org/10.5435/00124635-201009000-00003>
 7. Brandon, M.L., Haynes, P.T., Bonamo, J.R., Flynn, M.I., Barrett, G.R. & Sherman, M.F. (2006) The association between posterior-inferior tibial slope and anterior cruciate ligament insufficiency. *Arthroscopy: The Journal of Arthroscopic & Related Surgery*, 22, 894–899. Available from: <https://doi.org/10.1016/j.arthro.2006.04.098>
 8. Christensen, J.J., Krych, A.J., Engasser, W.M., Vanhees, M.K., Collins, M.S. & Dahm, D.L. (2015) Lateral tibial posterior slope is increased in patients with early graft failure after anterior cruciate ligament reconstruction. *The American Journal of Sports Medicine*, 43, 2510–2514. Available from: <https://doi.org/10.1177/0363546515597664>
 9. Dare, D.M., Fabricant, P.D., McCarthy, M.M., Rebolledo, B.J., Green, D.W., Cordasco, F.A. et al. (2015) Increased lateral tibial slope is a risk factor for pediatric anterior cruciate ligament injury: an MRI-based case-control study of 152 patients. *The American Journal of Sports Medicine*, 43, 1632–1639. Available from: <https://doi.org/10.1177/0363546515579182>
 10. Dejour, H. & Bonnin, M. (1994) Tibial translation after anterior cruciate ligament rupture. Two radiological tests compared. *The Journal of Bone and Joint Surgery. British Volume*, 76-B, 745–749. Available from: <https://doi.org/10.1302/0301-620X.76B5.8083263>
 11. Duerr, R., Ormseth, B., Adelstein, J., Garrone, A., DiBartola, A., Kaeding, C. et al. (2023) Elevated posterior tibial slope is associated with anterior cruciate ligament reconstruction failures: a systematic review and meta-analysis. *Arthroscopy: The Journal of Arthroscopic & Related Surgery*, 39, 1299–1309.e6. Available from: <https://doi.org/10.1016/j.arthro.2022.12.034>
 12. Giffin, J.R., Vogrin, T.M., Zantop, T., Woo, S.L.Y. & Harner, C.D. (2004) Effects of increasing tibial slope on the biomechanics of the knee. *The American Journal of Sports Medicine*, 32, 376–382. Available from: <https://doi.org/10.1177/0363546503258880>
 13. Grassi, A., Macchiarola, L., Urrizola Barrientos, F., Zicaro, J.P., Costa Paz, M., Adravanti, P. et al. (2019) Steep posterior tibial slope, anterior tibial subluxation, deep posterior lateral femoral condyle, and meniscal deficiency are common findings in multiple anterior cruciate ligament failures: an MRI case-control study. *The American Journal of Sports Medicine*, 47, 285–295. Available from: <https://doi.org/10.1177/0363546518823544>
 14. Grassi, A., Signorelli, C., Urrizola, F., Macchiarola, L., Raggi, F., Mosca, M. et al. (2019) Patients with failed anterior cruciate ligament reconstruction have an increased posterior lateral tibial plateau slope: a case-controlled study. *Arthroscopy: The Journal of Arthroscopic & Related Surgery*, 35, 1172–1182. Available from: <https://doi.org/10.1016/j.arthro.2018.11.049>
 15. Hashemi, J., Chandrashekar, N., Gill, B., Beynnon, B.D., Slauterbeck, J.R., Schutt Jr., R.C. et al. (2008) The geometry of the tibial plateau and its influence on the biomechanics of the tibiofemoral joint. *The Journal of Bone and Joint Surgery-American Volume*, 90, 2724–2734. Available from: <https://doi.org/10.2106/JBJS.G.01358>
 16. Hohmann, E., Tetsworth, K., Glatt, V., Ngcelwane, M. & Keough, N. (2021) Medial and lateral posterior tibial slope are independent risk factors for noncontact ACL injury in both men and women. *Orthopaedic Journal of Sports Medicine*, 9, 23259671211015940. Available from: <https://doi.org/10.1177/23259671211015940>
 17. Hudek, R., Schmutz, S., Regenfelder, F., Fuchs, B. & Koch, P.P. (2009) Novel measurement technique of the tibial slope on conventional MRI. *Clinical Orthopaedics & Related Research*, 467, 2066–2072. Available from: <https://doi.org/10.1007/s11999-009-0711-3>
 18. Kataoka, K., Nagai, K., Hoshino, Y., Shimabukuro, M., Nishida, K., Kanzaki, N. et al. (2022) Steeper lateral posterior tibial slope and greater lateral-medial slope asymmetry correlate with greater preoperative pivot-shift in anterior cruciate ligament injury. *Journal of Experimental Orthopaedics*, 9, 117. Available from: <https://doi.org/10.1186/s40634-022-00556-x>
 19. Liu, Z., Jiang, J., Yi, Q., Teng, Y., Liu, X., He, J. et al. (2022) An increased posterior tibial slope is associated with a higher risk of graft failure following ACL reconstruction: a systematic review. *Knee Surgery, Sports Traumatology, Arthroscopy*, 30, 2377–2387. Available from: <https://doi.org/10.1007/s00167-022-06888-6>
 20. Lu, Y., Pareek, A., Yang, L., Rouzrokh, P., Khosravi, B., Okoroha, K.R. et al. (2023) Deep learning artificial intelligence tool for automated radiographic determination of posterior tibial slope in patients with ACL injury. *Orthopaedic Journal of Sports Medicine*, 11, 23259671231215820. Available from: <https://doi.org/10.1177/23259671231215820>
 21. Mandalia, V., Bayley, M., Bhamber, N., Middleton, S. & Houston, J. (2023) Posterior tibial slope in anterior cruciate ligament surgery: a systematic review. *Indian Journal of Orthopaedics*, 57, 1376–1386. Available from: <https://doi.org/10.1007/s43465-023-00947-x>
 22. Meier, M.P., Hochrein, Y., Saul, D., Seitz, M.T., Klockner, F.S., Lehmann, W. et al. (2022) Morphological analysis of the tibial slope in 720 adult knee joints. *Diagnostics (Basel, Switzerland)*, 12, 1346. Available from: <https://doi.org/10.3390/diagnostics12061346>
 23. Naendrup, J.H., Drouven, S.F., Shaikh, H.S., Jaecker, V., Offerhaus, C., Shafizadeh, S.T. et al. (2020) High variability of tibial slope measurement methods in daily clinical practice: comparisons between measurements on lateral radiograph, magnetic resonance imaging, and computed tomography. *The Knee*, 27, 923–929. Available from: <https://doi.org/10.1016/j.knee.2020.01.013>
 24. Narahashi, É., Guimarães, J.B., Filho, A.G.O., Nico, M.A.C. & Silva, F.D. (2024) Measurement of tibial slope using biplanar stereoradiography (EOS®). *Skeletal Radiology*, 53, 1091–1101. Available from: <https://doi.org/10.1007/s00256-023-04528-9>
 25. Petrigliano, F.A., Suero, E.M., Voos, J.E., Pearle, A.D. & Allen, A.A. (2012) The effect of proximal tibial slope on dynamic

- stability testing of the posterior cruciate ligament- and postero-lateral corner-deficient knee. *The American Journal of Sports Medicine*, 40, 1322–1328. Available from: <https://doi.org/10.1177/0363546512439180>
26. Rahnama-Azar, A.A., Abebe, E.S., Johnson, P., Labrum, J., Fu, F.H., Irrgang, J.J. et al. (2017) Increased lateral tibial slope predicts high-grade rotatory knee laxity pre-operatively in ACL reconstruction. *Knee Surgery, Sports Traumatology, Arthroscopy*, 25, 1170–1176. Available from: <https://doi.org/10.1007/s00167-016-4157-3>
 27. Shultz, S.J., Schmitz, R.J., Benjaminse, A., Collins, M., Ford, K. & Kulas, A.S. (2015) ACL Research retreat VII: An update on anterior cruciate ligament injury risk factor identification, screening, and prevention. *Journal of Athletic Training*, 50, 1076–1093. Available from: <https://doi.org/10.4085/1062-6050-50.10.06>
 28. Smith, H.C., Vacek, P., Johnson, R.J., Slauterbeck, J.R., Hashemi, J., Shultz, S. et al. (2012) Risk factors for anterior cruciate ligament injury: a review of the literature - part 1: neuromuscular and anatomic risk. *Sports Health: A Multidisciplinary Approach*, 4, 69–78. Available from: <https://doi.org/10.1177/1941738111428281>
 29. Tensho, K., Kumaki, D., Yoshida, K., Shimodaira, H., Horiuchi, H. & Takahashi, J. (2023) Does posterior tibial slope laterality exist? A matched cohort study between ACL-injured and non-injured knees. *Journal of Experimental Orthopaedics*, 10, 132. Available from: <https://doi.org/10.1186/s40634-023-00702-z>
 30. Todd, M.S., Lalliss, S., Garcia, E., DeBerardino, T.M. & Cameron, K.L. (2010) The relationship between posterior tibial slope and anterior cruciate ligament injuries. *The American Journal of Sports Medicine*, 38, 63–67. Available from: <https://doi.org/10.1177/0363546509343198>
 31. Tong, L., Xue, S., Chen, X. & Fang, R. (2023) Artificial intelligence-based detection of posterior tibial slope on X-ray images of unicompartmental knee arthroplasty patients. *Journal of Radiation Research and Applied Sciences*, 16, 100615. Available from: <https://doi.org/10.1016/j.jrras.2023.100615>
 32. Utzschneider, S., Goettinger, M., Weber, P., Horng, A., Glaser, C., Jansson, V. et al. (2011) Development and validation of a new method for the radiologic measurement of the tibial slope. *Knee Surgery, Sports Traumatology, Arthroscopy*, 19, 1643–1648. Available from: <https://doi.org/10.1007/s00167-011-1414-3>
 33. Wang, Y., Yang, T., Zeng, C., Wei, J., Xie, D., Yang, Y. et al. (2017) Association between tibial plateau slopes and anterior cruciate ligament injury: a meta-analysis. *Arthroscopy: The Journal of Arthroscopic & Related Surgery*, 33, 1248–1259.e4. Available from: <https://doi.org/10.1016/j.arthro.2017.01.015>
 34. Wen, D., Bohlen, H. & Wang, D. (2023) Paper 24: reliability of posterior tibial slope measurement on magnetic resonance imaging versus computed tomography. *Orthopaedic Journal of Sports Medicine*, 11, 2325967123S2325900050. Available from: <https://doi.org/10.1177/2325967123S000050>
 35. Wordeman, S.C., Quatman, C.E., Kaeding, C.C. & Hewett, T.E. (2012) In vivo evidence for tibial plateau slope as a risk factor for anterior cruciate ligament injury: a systematic review and meta-analysis. *The American Journal of Sports Medicine*, 40, 1673–1681. Available from: <https://doi.org/10.1177/0363546512442307>
 36. Zeng, C., Cheng, L., Wei, J., Gao, S., Yang, T., Luo, W. et al. (2014) The influence of the tibial plateau slopes on injury of the anterior cruciate ligament: a meta-analysis. *Knee Surgery, Sports Traumatology, Arthroscopy*, 22, 53–65. Available from: <https://doi.org/10.1007/s00167-012-2277-y>
 37. Zhang Y., Chen Y., Qiang M., Zhang K., Li H., Jiang Y., et al. (2018) Comparison between three-dimensional CT and conventional radiography in proximal tibia morphology. *Medicine* 97, e11632. <https://doi.org/10.1097/md.00000000000011632>

How to cite this article: Yao, S.-Y., Zhang, X.-Z., Podder, S., Wu, C.-T., Chan, Y.-S., Berco, D. et al. (2024) Enhanced reliability and time efficiency of deep learning-based posterior tibial slope measurement over manual techniques. *Knee Surgery, Sports Traumatology, Arthroscopy*, 1–11. <https://doi.org/10.1002/ksa.12241>